Initial Research on Stability Margin of Nonlinear Systems under Additive-State-Decomposition-Based Control Framework

Jin-Rui Ren, Quan Quan
School of Automation Science and Electrical Engineering, Beihang University, Beijing, 100191, China
E-mail: renjinrui@buaa.edu.cn; qq_buaa@buaa.edu.cn

Abstract: The study on the stability margin of nonlinear systems is difficult and meaningful. This paper makes an initial research on the stability margin for a nonlinear system with the unmodeled higher-order uncertainty. Three stabilizing control methods are tried, and the additive-state-decomposition-based control is the best compared with the other two. The first control method is the feedback linearization control, which may lead to a singularity problem. To avoid the singularity, a backstepping controller is further designed. However, it is still hard to analyze the system stability margin due to the nonlinearity. For such a purpose, the third control method, namely additive-state-decomposition-based control, is proposed to overcome both problems above. Under the additive-state-decomposition-based control framework, the stability margin of the nonlinear system is studied by the Bode plot method, which can be realized via a data-driven method. Finally, a series compensator is designed to compensate for the unmodeled higher-order uncertainty, and make the system stability margin satisfy the design specification. The comparison of the three methods and the verification of the validity of stability margin are illustrated by the simulation.

Key Words: Nonlinear systems, Stability margin, Feedback linearization, Backstepping, Additive state decomposition, Bode plot, Singularity, Data-driven

1 INTRODUCTION

Uncertainty and nonlinearity are two main difficulties in controller design, and they are inevitable for almost all practical systems. The uncertainty, such as delay or unmodeled higher-order dynamics, can be better considered by the concept of stability margin, i.e., amplitude and phase margins [1]. The stability margin of a system can be obtained by the Bode plot or Nyquist plot of the system. The Bode plot method is the first choice in practical engineering and it can be further acquired through sine sweep experiments [2]-[3], as presented in Fig.1, which can be viewed as a data-driven method. Sweep signals stimulate at the point B as the input, with the output responses being collected at the point A. Through the obtained input-output data, the corresponding Bode plot can be drawn. However, the Bode plot method is only applicable to linear systems, and cannot be used in nonlinear systems directly. Thus, it is hard to know the stability margin of nonlinear systems. What's more, stability margin makes sense only when the system is stable. Therefore, it is meaningful to study the stabilizing control and the stability margin for the systems with uncertainty and nonlinearity, which motivates us to carry out this initial research.

In this paper, the stabilizing control problem is investigated for a typical uncertain nonlinear system. Various stabilizing control methods have been applied to this system. Generally, there exist two major control methods to handle nonlinearity.

(i) Feedback Linearization Control (FLC) [4]. The key idea of FLC is transforming a nonlinear system into an equivalent linear system. Thus, stability margin can be adopted to analyze the stability of the linearized closed-loop system. Nevertheless, FLC may lead to a singularity problem, i.e., a vanishing denominator, which makes the system uncontrollable [5]. To avoid the singularity condition, the working state of the system must be greatly restricted, e.g., a saturating constraint was imposed to the control signal in [6].

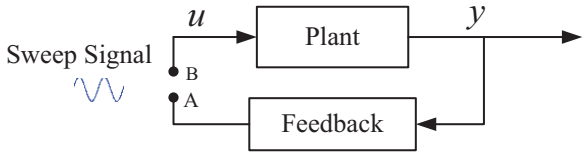

Figure 1: Sine sweep experiments.

(ii) Backstepping Control (BC) [7]. BC is a stabilizing control technique for a class of nonlinear systems with a recursive structure. The benefit of employing BC is that there is not the singularity problem. However, the ideal backstepping controller cannot be precisely obtained with unknown information in the system, and some other methods need to be considered additionally to improve or replace BC [8]-[9]. Further, because of the inapplicability of the Bode plot method for nonlinear systems, it is hard to handle the uncertainty.

To utilize the advantages of the two control methods mentioned above, a third control method, named as additive-state-decomposition-based control (ASDC) [10]-[11], is proposed. The central idea of ASDC is that the original

This work is supported by National Natural Science Foundation of China (No. 61473012,51375462).

nonlinear system is decomposed into a linear time-invariant (LTI) 'primary' system with all the uncertainty and a nonlinear 'secondary' system by additive state decomposition (ASD) [11]. Then, stabilizing controllers are separately designed for the primary and secondary systems as follows:

(i) For the LTI component, a linear stabilizing controller is designed by state feedback. Based on the stabilizing control, uncertainty is analyzed by the Bode plot method and stability margin is introduced. A series compensator is further designed to compensate for the uncertainty and make the stability margin of the system satisfy the frequency-domain design specification.

(ii) For the nonlinear component, a nonlinear stabilizing controller is designed by using BC to handle nonlinearity and avoid singularity.

By combining the two parts, the original control goal is achieved.

2 PROBLEM FORMULATION

To make the initial research reader-friendly, this paper considers two simple nonlinear systems as study objects. One is a nominal system without uncertainty and the other is an uncertain system.

(i) First, consider a nominal model as follows:

$$\begin{aligned} \dot{x}_1 &= a \sin x_2 \\ \dot{x}_2 &= k_1 x_1 + k_2 x_2 + u, \end{aligned} \tag{1}$$

where $x_1, x_2 \in \mathbb{R}$ are the states, $u \in \mathbb{R}$ is the control input, and a, k_1, $k_2 \in \mathbb{R}$ are known constants. The system (1) is an uncertainty-free nonlinear system, based on which the stabilizing controllers are designed in the following.

(ii) Based on (1), consider an uncertain model as follows:

$$\begin{aligned} \dot{x}_1 &= a \sin x_2 \\ \dot{x}_2 &= k_1 x_1 + k_2 x_2 + u_\xi, \end{aligned} \tag{2}$$

here,

$$u_\xi(s) = (1 + \Delta(s))\, u(s), \tag{3}$$

where $\Delta(s) = \frac{\omega_n^2}{s^2 + 2\omega_n \xi s + \omega_n^2} e^{-\tau s} - 1$ with $\omega_n, \tau > 0$. The system (2) is a nonlinear system with the unmodeled higher-order uncertainty in the input channel. The system (2) cannot be obtained directly. However, its input-output data can be acquired in practice. The system (2) is considered to highlight the advantages of ASDC and make a comparison among the control methods used in this paper. The following assumptions about the systems (1) and (2) are made.

Assumption 1. The system (1) is stable.

Assumption 2. The state $x = [x_1\ x_2]^{\mathrm{T}}$ is measurable.

The objectives of this paper are (i) design stabilizing controllers for the systems (1) and (2) to improve the system performance; (ii) under the ASDC framework, study the stability margin of the system (2) by the Bode plot method; (iii) in terms of the obtained Bode plot, design a series compensator for the system (2) to compensate for the uncertainty.

3 EXISTING CONTROL METHODS AND DRAWBACKS

In this section, two existing control methods, namely the FLC method and the BC method, are applied to the system (1). On the whole, the two existing control methods can only fulfill the objective (i). The concrete design is proposed in the following.

3.1 FLC Method

For the system (1), define a new state variable $x_2' = \sin x_2$. Then, the system (1) becomes

$$\begin{aligned} \dot{x}_1 &= a x_2' \\ \dot{x}_2' &= \cos x_2 \,(k_1 x_1 + k_2 x_2) + \cos x_2 u. \end{aligned} \tag{4}$$

A state feedback controller is designed via a linear quadratic regulator (LQR) for the system (4) as follows:

$$u = \frac{1}{\cos x_2} \left(-\cos x_2 \,(k_1 x_1 + k_2 x_2) + l_1 x_1 + l_2 x_2'\right). \tag{5}$$

Substituting (5) into (4) results in

$$\begin{aligned} \dot{x}_1 &= a x_2' \\ \dot{x}_2' &= l_1 x_1 + l_2 x_2', \end{aligned} \tag{6}$$

which is a linear system.

Remark 1. Since the original system (1) has been linearized to the system (6), the stability margin of the closed-loop system (6) can be obtained by the Bode plot method. However, there exists a singularity problem that the system (6) becomes uncontrollable when $x_2 = \pi/2 \pm k\pi$, $k = 1, 2, 3, \cdots$, i.e., $\cos x_2 = 0$. Additionally, there are more than one equilibrium position, which means that the steady state of the system may differ because of the different choices of initial values and the influence of uncertainty.

3.2 BC Method

For the system (1), define a new state variable $x_2' = x_2 + b \arctan x_1$. Then, the system (1) becomes

$$\begin{aligned} \dot{x}_1 &= a \sin(-b \arctan x_1 + x_2') \\ \dot{x}_2' &= \dot{x}_2 + b \tfrac{1}{x_1^2+1} \dot{x}_1 \\ &= k_1 x_1 + k_2 x_2 + u + b \tfrac{1}{x_1^2+1} a \sin x_2. \end{aligned} \tag{7}$$

A backstepping controller is designed for the system (7) as follows:

$$u = -(k_1 x_1 + k_2 x_2) - b \frac{1}{x_1^2 + 1} (a \sin x_2) - c x_2'. \tag{8}$$

Substituting (8) into (7), the following system is obtained

$$\begin{aligned} \dot{x}_1 &= a \sin(-b \arctan x_1 + x_2') \\ \dot{x}_2' &= -c x_2'. \end{aligned} \tag{9}$$

Remark 2. The singularity problem is avoided through adopting BC. Nevertheless, the closed-loop system (9) is nonlinear, and the stability margin of which is hard to be analyzed via the Bode plot method. Thus, by following the similar idea, the controller design for the system (2) becomes difficult.

4 ASDC METHOD

In order to avoid the limitations of the two control methods above, a new control method is introduced in this section. Based on the new method, the singularity problem is avoided and the system stability margin can be analyzed via the Bode plot method.

4.1 ASD for System (1)

The system (1) is rewritten as:

$$\begin{aligned} \dot{x}_1 &= ax_2 + (a\sin x_2 - ax_2) \\ \dot{x}_2 &= k_1x_1 + k_2x_2 + u. \end{aligned} \tag{10}$$

The system (10) can be generally expressed as $\dot{x} = f(t,x)$. Considering the system (10) as the original system. According to ASD mentioned in [10], the primary system is chosen as follows:

$$\begin{aligned} \dot{x}_{1,p} &= ax_{2,p} \\ \dot{x}_{2,p} &= k_1x_{1,p} + k_2x_{2,p} + u_p, x_p(0) = x(0), \end{aligned} \tag{11}$$

where $x_p = [x_{1,p}\ x_{2,p}]^{\mathrm{T}}$. The system (11) can be generally expressed as $\dot{x}_p = f_p(t,x_p)$. Define a new variable $x_s = [x_{1,s}\ x_{2,s}]^{\mathrm{T}} = x - x_p$. Then, the secondary system is determined by subtracting the primary system (11) from the original system (10):

$$\dot{x}_s = \dot{x} - \dot{x}_p = f(t,x) - f_p(t,x_p),$$

that is

$$\begin{aligned} \dot{x}_{1,s} &= ax_{2,s} + (a\sin(x_{2,p}+x_{2,s}) - a(x_{2,p}+x_{2,s})) \\ \dot{x}_{2,s} &= k_1x_{1,s} + k_2x_{2,s} + u_s, x_s(0) = 0, \end{aligned} \tag{12}$$

where $u_s = u - u_p$ and $(x_s, u_s) = (\mathbf{0}_{2\times1}, 0)$ is an equilibrium point of the system (12). According to ASD, we have

$$\begin{aligned} x &= x_p + x_s \\ u &= u_p + u_s. \end{aligned} \tag{13}$$

From (10)-(12), it can be seen that if the controller u_p drives $x_p \to 0$ as $t \to \infty$ and the controller u_s drives $x_s \to 0$ as $t \to \infty$, then $x \to 0$ as $t \to \infty$. The strategy here is to assign the linear stabilizing task to the primary system (11) and the nonlinear stabilizing task to the secondary system (12), which is shown in Fig.2. As a classical LTI system, the standard time-domain or frequency-domain linear control methods are applicable to the primary system (11). On the other hand, the standard nonlinear control methods can be adopted to the secondary system (12).

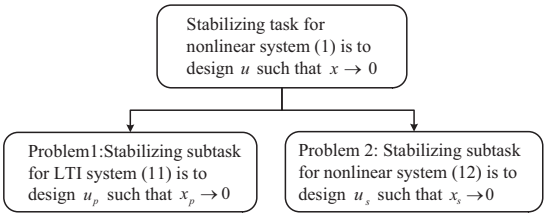

Figure 2: Additive state decomposition of the system (1).

4.2 Stabilizing Controller Design for System (1)

Until now, the original system (10) has been decomposed into two subsystems in charge of the corresponding subtasks. Then, controllers are designed in terms of two problems with respect to the two subtasks, respectively.

Problem 1. *Design u_p to make x_p bounded and $x_p \to 0$ as $t \to \infty$.*

Similar to Section 3.1, a LQR-based state feedback controller for (11) is designed as

$$u_p = -(k_1x_{1,p} + k_2x_{2,p}) + (l_1x_{1,p} + l_2x_{2,p}). \tag{14}$$

It can be written in the form of transfer function as $u_p(s) = p^T x_p(s)$, where $p \in \mathbb{R}^2$ is the state feedback gain matrix.

Remark 3. Based on *Assumptions 1&2*, suppose the controller for (11) is designed as (14). Then x_p is bounded and $x_p \to 0$ as $t \to \infty$.

Problem 2. *Design u_s to drive $x_s \to 0$ when $x_p \to 0$ as $t \to \infty$.*

The secondary system (12) is rewritten as:

$$\begin{aligned} \dot{x}_{1,s} &= a\sin(x_{2,s}) + g \\ \dot{x}_{2,s} &= k_1x_{1,s} + k_2x_{2,s} + u_s, \end{aligned}$$

where $g = a(\sin(x_{2,p}+x_{2,s}) - \sin(x_{2,s})) - ax_{2,p}$. Similar to Section 3.2, a backstepping controller is designed as

$$\begin{aligned} u_s \quad = \quad & -(k_1x_{1,s} + k_2x_{2,s}) - \\ & b\tfrac{1}{x_{1,s}^2+1}(a\sin x_{2,s} + g) - cx'_{2,s}, \end{aligned} \tag{15}$$

where $x'_{2,s} = x_{2,s} + b\arctan x_{1,s}$.

Remark 4. If the primary system is stable, then $g \to 0$. Consequently, $x_s \to 0$.

Note that x_p and x_s are virtual states, which are unknown. Then, an observer is designed to estimate x_p and x_s, as shown in *Theorem 1*.

Theorem 1. Suppose that an observer is designed to estimate states x_p and x_s in (11)-(12) as follows:

$$\begin{cases} \dot{\hat{x}}_{1,s} = a\hat{x}_{2,s} + (a\sin(x_2) - ax_2) \\ \dot{\hat{x}}_{2,s} = k_1\hat{x}_{1,s} + k_2\hat{x}_{2,s} + u_s \end{cases}, \hat{x}_s(0) = 0, \tag{16}$$

and

$$\begin{cases} \hat{x}_{1,p} = x_1 - \hat{x}_{1,s} \\ \hat{x}_{2,p} = x_2 - \hat{x}_{2,s}. \end{cases} \tag{17}$$

Then $\hat{x}_p \equiv x_p$ and $\hat{x}_s \equiv x_s$.

Proof. Similar to [11]. □

Theorem 2. Based on *Assumptions 1&2*, suppose (i) *Problems 1&2* are solved; (ii) the controller for the system (1) is designed as

$$u \quad = \quad u_p(\hat{x}_p) + u_s(\hat{x}_s, \hat{x}_p). \tag{18}$$

Then, the closed-loop system of the system (1) with the controller (18) satisfies $x \to 0$ as $t \to \infty$.

Proof. Similar to [11]. □

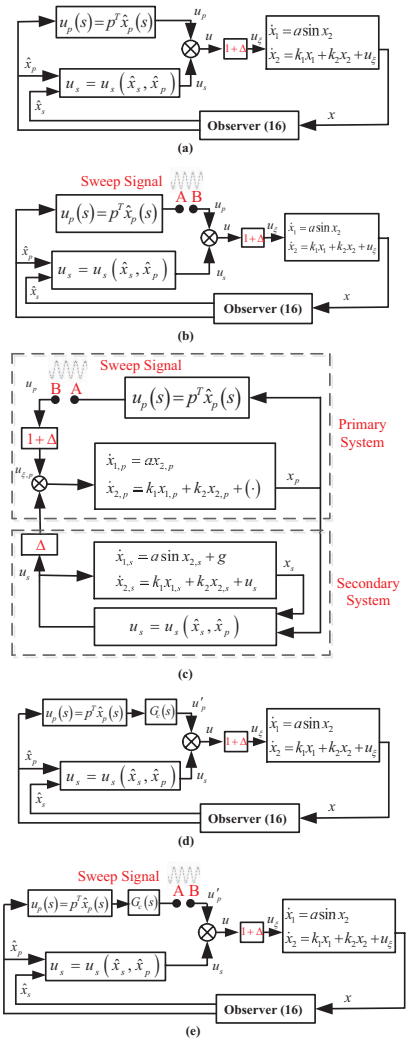

Figure 3: The structure of the closed-loop control systems and the design of sine sweep experiments. Fig.3 (a) shows the closed-loop system of the system (2) with the controller (18). Its corresponding sine sweep experiments are presented in Fig.3 (b), which is equivalent to Fig.3 (c) for analysis. Fig.3 (d) depicts the closed-loop system of the system (2) with the controller (20). Its corresponding sine sweep experiments are presented in Fig.3 (e). Sweep sine signals stimulate at the point B as the input, with the output responses being collected at the point A in Fig.3 (b),(c),(e).

4.3 Stability Margin Analysis for System (2)

At first, the controller (18) is directly applied to the system (2). The structure of the closed-loop control system is presented in Fig.3 (a).

(i) *Approximate feasibility of the Bode plot method under the ASDC framework*

As we know, the Bode plot method is inapplicable to nonlinear systems directly. However, the Bode plot method is approximately applicable under the proposed ASDC framework. As shown in Fig.3 (c), if $\Delta = 0$, then the secondary system has no input to the primary system. As a result, the primary system is linear; Furthermore, if $\Delta \neq 0$, then $\Delta \cdot u_s$ will be an external signal added into the primary system. From the definition of $\Delta(s)$, the term $\Delta \cdot u_s$ can be ignored when the frequency ω is low or the delay time constant τ is small. Then, the primary system can be approximately viewed as a linear system. Based on this, the Bode plot method is approximately applicable to the primary system. On the other hand, the secondary system (12) is certain, leaving all the uncertainty in the primary system. Thus, it is reasonable to only study the primary system. The stability margin for the whole system can be presented in terms of the Bode plot of the primary system. The simulation study then also verifies the above analysis.

(ii) *Verification of the stability margin of system (2)*

It was shown in the previous subsection (i) that the Bode plot method is approximately applicable to the linear primary system. Conversely, the obtained Bode plot can also show whether the primary system is linear [1]. The validity of the stability margin can be verified through confirming that the primary system is linear by the Bode plot.

i) Through changing the delay time constant τ of the system and observing the change of the Bode plot, the correctness of the obtained phase margin γ can be verified.

ii) Through changing the open-loop gain k of the system and observing the change of the Bode plot, the correctness of the obtained amplitude margin h can be verified.

iii) The largest delay time constant which the system can tolerate, namely τ_m, is also derivable. τ_m is a very significant parameter in practice, and there are two approaches to calculate it. Theoretically, if the system is linear, then $\tau_m = \frac{\gamma(rad)}{\omega_c}$, where ω_c is cutoff frequency. On the other hand, τ_m can be experimentally determined by increasing τ until $h = 0$.

The methods above will be used to verify the obtained stability margin of the system (2) in the simulation.

4.4 Series Compensator Design for System (2)

To improve the system response through compensating for the uncertainty in the primary system, the series compensation is further considered [1]. As shown in Fig.3 (b), through the sine sweep experiments of the system (2) with the designed controller (18), a Bode plot is obtained. Based on this Bode plot, a series compensator is designed as

$$G_c(s) = \frac{1+\beta Ts}{1+Ts},$$

where $\beta < 1$. Then, the controller for the primary system of the system (2) is changed to

$$\begin{aligned} u_p'(s) &= G_c(s)\, u_p(s) \\ &= \tfrac{1+\beta Ts}{1+Ts} p^T x_p(s). \end{aligned} \tag{19}$$

Keeping the controller (15) for the secondary system unchanged, the controller for the system (2) is finally designed as

$$u = u_p'(\hat{x}_p) + u_s(\hat{x}_s, \hat{x}_p). \tag{20}$$

The structure of the final closed-loop control system is presented in Fig.3 (d).

5 SIMULATION STUDY AND DISCUSSIONS

In this section, the performance of the three proposed control methods is compared through the time-domain simulation. Meanwhile, the effectiveness of series compensation and the validity of the stability margin based on the Bode plot are presented through the frequency-domain simulation.

5.1 Parameters Setting

Let $x(0) = [1\ 1]^{\mathrm{T}}$. The system parameters are selected as $a = 1$, $k_1 = 0$, $k_2 = 1$. The parameters of the uncertainty are assigned as $\omega_n = 5$, $\xi = 0.5$, $\tau = 0.05$, i.e., $\Delta(s) = \frac{25}{s^2+5s+25}e^{-0.05s} - 1$. For FLC, the state feedback gain matrix is determined by the LQR method as $l_1 = -3.1623$, $l_2 = -4.0404$ when $R = 1$ and $Q = \mathrm{diag}(10, 10)$. For BC, the controller parameters are selected as $b = 1$, $c = 3$. For ASDC, the parameters for the primary system controller are selected the same as those of FLC, and the parameters for the secondary system controller are selected the same as those of BC. The frequency-domain design specification for series compensation is set as $\omega_c \geq 1\,(rad/s)$, $\gamma \geq 60\,(^\circ)$, $h \geq 6\,(dB)$. The series compensator is designed as $G_c(s) = \frac{1+6.63s}{1+14.03s}$, that is $\beta = 0.4723$, $T = 14.03$.

5.2 Time-domain Simulation Results

For FLC and BC, two systems are considered, namely the system (1) and the system (2). For ASDC, three closed-loop systems are considered as follows:
(i) Case 1. the system (1) with the controller (18).
(ii) Case 2. the system (2) with the controller (18).
(iii) Case 3. the system (2) with the controller (20).

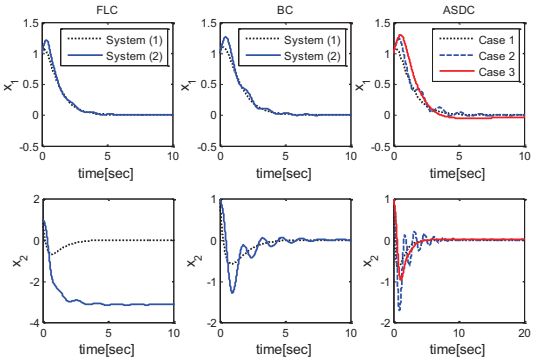

Figure 4: State responses with FLC, BC and ASDC.

The system state responses with FLC, BC and ASDC are presented in Fig.4. For the system (1), the performance under the three controllers is similar. However, when the system (2) is considered, the performance under all three controllers gets worse. For ASDC, the controller for the system (2) is redesigned as (20), so the performance is improved in Case 3. For FLC, system states are stable in the end but cannot return to the equilibrium point $x = [0\ 0]^{\mathrm{T}}$. A comparison about time-domain responses for the system (2) among the three methods is illustrated in Fig.5. ASDC provides better response than the other two. The control input of FLC has a peak at one particular moment, which

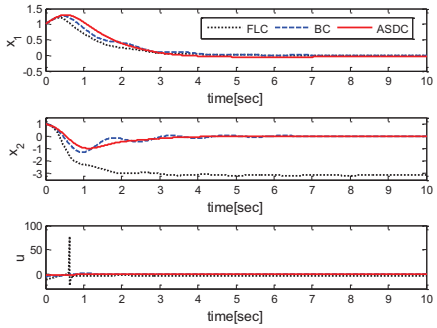

Figure 5: States and control inputs of the system (2) with FLC, BC and ASDC. For ASDC, Case 3 is considered.

corresponds to the singularity.

5.3 Frequency-domain Simulation Results

To show the effectiveness of the designed series compensator by comparison, the three cases as Section 5.2 are considered. It can be found from Fig.6 and Table.1

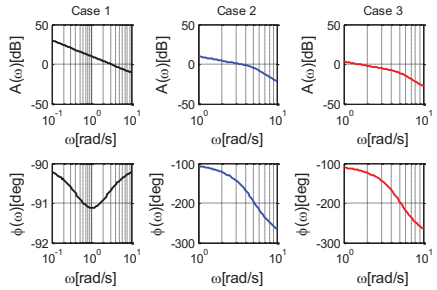

Figure 6: Bode plots of the three closed-loop systems.

Table 1: Frequency-domain stability analysis results.

		$\omega_c\,(rad/s)$	$\gamma\,(^\circ)$	$h\,(dB)$
Design specification		≥ 1	≥ 60	≥ 6
Actual performance	Case 1	3.05	90	Inf
	Case 2	3.5	25	2.5
	Case 3	1.5	64	9

(i) the stability margin of Case 1 is very high, and exceeds the specification. However, it should be pointed out that the system (1) in Case 1 is uncertainty-free.
(ii) When the uncertainty is considered, the stability margin of Case 2 gets worse, and falls short of the specification. Thus, the unmodeled higher-order uncertainty decreases the system stability.
(iii) After the series compensator is added into the system (2), the stability margin of Case 3 becomes much better again, and satisfies the specification. Thus, the series compensator compensates the uncertainty very well.
According to the subsection 4.3(ii), some tests are further carried out to verify the validity of the obtained stability margin of the closed-loop system in Case 3, the corresponding sine sweep experiments are depicted in Fig.3 (e).

(i) To verify the phase margin γ, the delay time constant is increased by $\tau = \tau_0 + \Delta\tau$. As shown in Fig.7, the amplitude frequency curve remains unchanged but the phase fre-

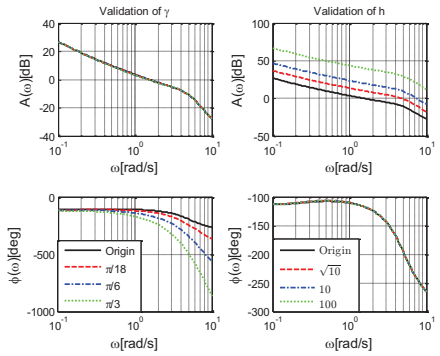

Figure 7: Validation test results of phase margin γ and amplitude margin h. Here $\Delta\tau = 0, \pi/18, \pi/6, \pi/3$ and $\Delta k = 0, \sqrt{10}, 10, 100$.

quency curve moves down. The phase change $\Delta\phi(rad) = \phi - \phi_0$ satisfies that $\Delta\phi = -\Delta\tau \cdot \omega$. It is concluded that the phase margin matches the linear property very well.
(ii) To verify the amplitude margin h, the system open-loop gain is increased by $k = k_0 \cdot \Delta k$. As shown in Fig.7, the phase frequency curve remains unchanged but the amplitude frequency curve overall moves up. The amplitude change $\Delta A\ (dB) = A - A_0$ satisfies that $\Delta A = 20\text{lg}(\Delta k)$. It is concluded that the amplitude margin matches the linear property very well.
(iii) Through the two approaches mentioned in Section 4.3, the simulation result is $\tau_m = 0.75$ and the theoretical result is $\tau_m = 0.745$, which are basically the same.
Observed from the results above, the change of the Bode plot matches the linear property very well. Thus, the primary system can be considered as a linear system. The stability margin of the primary system can feature the stability of the whole system.

5.4 Discussions

From the simulation results, it can be seen that ASDC provides a better time-domain response for the system (2). Moreover, ASDC makes the Bode plot based stability margin applicable to the original nonlinear system. The proposed ASDC method is similar to a two-degree-of-freedom control, i.e., the problem can be decomposed into two separate parts, which facilitates the design. When considering the uncertainty of a nonlinear system, i.e., changing the system (1) to the system (2), a series compensator is added to the primary system and the controllers designed for the system (1) are totaly retained, which is convenient in practical applications. The advantages and disadvantages of the three methods are summarized in Table.2.

6 CONCLUSIONS

In this paper, an initial research on stability margin for an uncertain nonlinear system under the ASDC framework is carried out. For comparison, the two existing methods, i.e., the FLC method and the BC method are also described. The simulation results demonstrate the effectiveness of the proposed controllers and the validity of stability margin. Our principal contributions lie on two respects. (i) A decomposition named ASD is introduced. The existing control methods can still be used to design controllers for the decomposed primary and secondary systems, and the drawbacks of the existing control methods are avoided in this way. Uncertainty and nonlinearity are separated into two subsystems, which mitigates the design difficulty of stabilizing control. (ii) Under the ASDC framework, the data-driven Bode plot method is approximately applicable to analyze the stability margin of the original nonlinear system. The range of application of stability margin is extended from linear systems to simple nonlinear systems, which acts as a stepping stone into the further work on the nonlinear stability margin. More complex and more practical systems will be analyzed in future research.

Table 2: Advantages and disadvantages of the three control methods.

	Advantages	Disdvantages
FLC	Linearized system; Applicability of stability margin	Singularity problem; More than one equilibrium point
BC	Singularity-free	Inapplicability of stability margin
ASDC	Singularity-free; Applicability of stability margin	Somewhat complicated

REFERENCES

[1] R. C. Dorf and R. H. Bishop, Modern Control Systems, 12th edition, Prentice-Hall, Englewood Cliffs, 2010.
[2] A. S. Cherry, R. P. Jones, and T. E. C. Potter, The use of multibody system modeling and multivariable system decoupling techniques in vehicle ride control, Journal of dynamic systems, measurement, and control, Vol.121, No.3, 479-486, 1999.
[3] S. Shinoda, K. Yubai, D. Yashiro, et al., Multivariable controller design evaluating closed-loop interaction by iterative LMI optimization using frequency response data, in Proc. of 2015 International Conference on Advanced Mechatronic Systems, 429-434, 2015.
[4] A. Isidori, Nonlinear Control Systems, 3rd edition, Springer Verlag, London, 1995.
[5] J. Ghosh and B. Paden, Nonlinear repetitive control, IEEE Transactions on Automatic Control, Vol.45, No.5, 949-954, 2000.
[6] A. Alasty and H. Salarieh, Nonlinear feedback control of chaotic pendulum in presence of saturation effect, Chaos, Solitons & Fractals, Vol.31, No.2, 292-304, 2007.
[7] P. V. Kokotovic, The joy of feedback: nonlinear and adaptive, Control Systems, IEEE, Vol.12, No.3, 7-17, 1992.
[8] C. F. Hsu, C. M. Lin, and T. T. Lee, Wavelet adaptive backstepping control for a class of nonlinear systems, IEEE Transactions on Neural Networks, Vol.17, No.5, 1175-1183, 2006.
[9] X. Gong, Z. C. Hou, C. J. Zhao, Y. Bai, and Y. T. Tianet, Adaptive backstepping sliding mode trajectory tracking control for a quad-rotor, International Journal of Automation and Computing, Vol.9, No.5, 555-560, 2012.
[10] Q. Quan, K. Y. Cai, and H. Lin, Additive-state-decomposition-based tracking control framework for a class of nonminimum phase systems with measurable nonlinearities and unknown disturbances, International Journal of Robust and Nonlinear Control, Vol.25, No.2, 163-178, 2015.
[11] Q. Quan and K. Y. Cai, Additive-state-decomposition-based tracking control for TORA benchmark, Journal of Sound and Vibration, Vol.332, No.20, 4829-4841, 2013.